Proteome and microbiota analysis reveals alterations of liver-gut axis under different stocking density of Peking ducks

Yuqin Wu,[†] Jianhui Li,[§] Xin Qin,[§] Shiqiang Sun,[†] Zhibin Xiao,[†] Xiaoyu Dong,[†] Muhammad Suhaib Shahid,[†] Dafei Yin,[†] Zhao Lei,[†] Yuming Guo,[†] Jianmin Yuan[*,†]

[†]State Key Laboratory of Animal Nutrition, College of Animal Science and Technology,

China Agricultural University, Beijing 100193, China

[§]College of Animal Science and Veterinary Medicine, Shanxi Agricultural University, Taigu 030801, China

*Corresponding author: Jianmin Yuan

Email: yuanjm@cau.edu.cn

Abstract

The aim of this study was to determine the impact of stocking density on the liver proteome and cecal microbiota of Peking ducks. A total of 1,200 ducks with 21-day old were randomly allotted into 5 stocking density groups of 5, 6, 7, 8 and 9 ducks/m^2, with 6 replicates for each group. At 40 days of age, duck serum and pectorals were collected for biochemical tests; liver and cecal contents of ducks were gathered for proteome and microbiota analysis, respectively. Serum MDA increased while pectorals T-AOC reduced linearly with enhancing stocking density. Duck lipid metabolism was altered under different stocking density as well. Serum LDL-C increased linearly with increasing stocking density. Proteome analysis revealed fatty acid biosynthesis proteins such as acyl-CoA synthetase family member 2 and fatty acid oxidation related proteins including acyl-CoA dehydrogenase long chain and acyl-coenzyme A oxidase were enriched in high stocking density group. Additionally, high stocking density increased oxidative response related proteins such as DDRGK domain containing 1 while diminished anti-oxidant capacity related proteins including regucalcin and catalase. 16S rDNA analysis revealed that higher stocking density was accompanied with decreased microbial diversity, as well as depletion of anti-inflammatory bacterial taxa, including *Bacteroidales, Butyricimonas* and *Alistipe*. In addition, decreased bile acid metabolism-associated bacteria such as *Ruminococcaceae, Clostridiales* and *Desulfovibrionaceae* were found in the high-density group. Both proteome and 16S rDNA results showed inflammation and chronic liver disease trend in the high-density group, which suggests the involvement of the liver-gut axis in oxidative stress.

Keywords: Duck; Stocking density; Stress; Proteome; Microbiota

INTRODUCTION

Space is one of the most compromised features in commercial housing systems, limited often in the interests of efficiency and profitability. Increasing stocking density can yield higher profits per kilogram of chicken. However, reduced space limits the ability to rest [1] and has a negative influence on performance [2,3,4,5,6], meat yield [2-4], immune status [7] and gut morphology [8]. In addition, high stocking density is associated with chronic oxidative stress [2].

The liver plays an important role in energy metabolism and it is the major site of triglyceride (TG) metabolism which is involved in TG digestion, absorption, synthesis, decomposition and transport. It has been demonstrated that high stocking density has been shown to have a deleterious effect on liver function [9] with increased activities with aspartate aminotransferase and alanine aminotransferase [10]. The gut microbiome is also highly connected to animal energy metabolism and health [11], and it has been frequently suggested that gut microbiota plays a critical role in chronic liver disorders through liver-gut axis [12]. Moreover, high stocking density is associated with adverse effects on the chicken intestinal commensal bacteria [4].

The emergence of novel proteomic techniques in recent years has greatly aided in the understanding of biological mechanisms. Tandem mass tag (TMT) [13] and isobaric tags for relative and absolute quantitation (iTRAQ) [14] methods have been widely used for analyzing the hepatic proteome. The TMT method can also be used to

characterize liver proteome-wide changes in response to oxidative stress [15]. Further, due to progress in high-throughput next-generation sequencing, 16S rDNA analysis can be used to infer the structure and function of gut microbiota.

To characterize the potential mechanism of oxidative stress under high stocking density, TMT-labeled quantitative proteomics combined with 16S rDNA analysis was used to identify changes in the protein profiles and microbiota of Peking ducks under low and high raising density.

MATERIALS AND METHODS

Ethics approval

All of our experiments were approved by the Institutional Animal Care and Use Committee of the China Agricultural University (Beijing, China).

Facilities and Experimental Animals

A total of 1200 mixed-sex 21-d-old white Peking ducks were randomly assigned to 5 stocking density treatments and 6 replicates. Each replicate corresponds one pen with 40 ducks (20 males, and 20 females). The raising area in different treatments were 8.20 m^2 (2.50 × 3.28 m), 6.88 m^2 (2.50 × 2.75 m), 5.93 m^2 (2.50 × 2.37 m), 5.20 m^2 (2.50 × 2.08 m) and 4.65 m^2 (2.5 × 1.86 m) and the corresponding stocking density was 5 (low stocking density represent as L group), 6, 7, 8, and 9 (high stocking density represent as H group) ducks/m^2, respectively. All ducks were raised in a plastic wire-floor pen and provided water and feed *ad libitum* from 21 to 40 d of age. In the house, lighting,

82 temperature and ventilation programs followed commercial practices. During the
83 experimental period, all ducks were raised with diets based on the NRC (1994) feeding
84 standard.

85 Growth Performance and Carcass Traits

86 Initial body weight (BW), final BW and feed intake (FI) were recorded. The weight
87 gain and feed/gain ratio were calculated.

88 Sample Collection

89 On day 40, one male duck per pen was randomly selected. Therefore, a total of 6
90 male ducks per treatment were collected. Each duck was sacrificed by stunning after
91 blood collection. The liver samples of ducks from L and H density treatments were
92 collected, flushed with cold PBS, frozen using liquid nitrogen, and stored at -80 °C for
93 and proteomic analysis. Cecum contents of ducks from L and H density treatments were
94 collected, transferred into Eppendorf tubes, and immediately frozen in liquid nitrogen
95 and stored at -80°C for microbiota analyses.

96 Abdominal fat and left pectorals of each duck were removed manually from the
97 carcass and weighed. For each duck, a piece of pectorals fixed position was separated
98 and put on the ice bag immediately, then stored at -80 °C for biochemical analysis.

99 Serum and Pectorals Biochemical Parameters

100 Serum levels of malondialdehyde (**MDA**, cat#A003-1), TG (cat#A110-2), total

cholesterol (**TC**, cat#A111-2), high-density lipoprotein cholesterol **(HDL-C**, cat#A112-2), low-density lipoprotein cholesterol (**LDL-C**, cat#A113-2), very low density lipoprotein (**VLDL**, cat#H249), total antioxidant capacity (**T-AOC**, cat#A015-1) and the activities of lactate dehydrogenase (**LDH**, cat#A020-1), creatine kinase (**CK**, cat#A032), glutamic-pyruvic transaminase (**GPT**, cat#C009-1), lipase (cat#A067), lipoprotein lipase (**LPL**, cat#A067) along with MDA, T-AOC, LPL and protein concentration (cat#A045-2) of pectorals were determined by using commercial analytical kits according to the manufacturer's recommendations (Jian Cheng Bioengineering Institute, Nanjing, China).

Statistical analysis.

One-way analysis of variance (ANOVA) models were fitted to assess the relationships between the stocking density groups and serum and pectoral redox and lipid metabolism indices, using SPSS (v.20.0, SPSS Institute, Chicago, IL). Means were compared using Duncan's multiple comparison procedure of SPSS software when density treatment was significant ($P < 0.05$), and curve estimation was used to assess the linear and quadratic effects of increasing stocking density on final body weight, body weight gain, feed gain ratio, and pectorals percentage. $P < 0.05$ was used for statistical significant and results were considered significant trend at $P < 0.1$.

Proteome analysis

Protein extraction

Liver samples (~100mg each) were ground to a powder under liquid nitrogen and then transferred into a centrifuge tube. After that, four times volume of lysis buffer containing 8 M urea (Sigma) and 1% Protease Inhibitor Cocktail (Calbiochem) was added, followed by sonication three times on ice using a high intensity ultrasonic processor (Scientz). And then centrifuged for 10 min at 4 °C and 12,000g. Supernatants containing soluble proteins were collected and the protein concentration was quantified with BCA kit (Beyotime Biotechnology) according to the manufacturer's instructions.

Trypsin digestion

For trypsin digestion, the protein solution was reduced with 5 mM dithiothreitol (Sigma) for 30 min at 56 °C and alkylated with 11 mM iodoacetamide (Sigma) for 15 min at room temperature under dark conditions. The protein sample was diluted with 100 mM triethylammonium bicarbonate (TEAB, Sigma) to make urea concentration less than 2 M. Finally, the sample was digested with trypsin (Promega) overnight with a 1:50 trypsin-to-protein ratio and then further digested for 4 h with 1:100 w: w trypsin-to-protein ratio (37℃).

TMT Labeling

After trypsin digestion, the peptides were desalted in a Strata X C18 SPE column (Phenomenex) and vacuum dried. The peptide was dissolved in 1 M TEAB and

processed according to the manufacturer's protocol for TMT kit. Briefly, one unit of TMT reagent (defined as the amount of reagent requirement for labeling 100 μg of protein) was thawed and dissolved in acetonitrile (Fisher Chemical). The peptide mixtures were then incubated for 2 h at room temperature, pooled, desalted and dried by vacuum centrifugation.

HPLC fractionation

Peptides were fractionated by high pH reverse-phase HPLC with an Agilent 300 Extend C18 column (5 μm particles, 4.6 mm ID, 250 mm length). Briefly, peptides were firstly separated by 8% to 32% acetonitrile (pH 9.0) over 60 minutes into 60 fractions. Subsequently, the peptides were combined into 18 fractions and dried by vacuum centrifugation.

Mass Spectrometry and TMT Data Analysis

Peptides were dissolved in 0.1% formic acid (Fluka), and separated by EASY-nLC 1000 UPLC system. Solvent A is an aqueous solution containing 0.1% formic acid and 2% acetonitrile; solvent B is an aqueous solution containing 0.1% formic acid and 90% acetonitrile. Liquid-phase gradient using a linearly increasing gradient of 5% to 24% solvent B for 38 min, 24% to 35% solvent B for 14 min, then climbing to 80% in 4 min, and then maintaining at 80% for the last 4 min, all at a constant flow rate of 800 nl/min.

The peptides results were subjected to nano electrospray ionization (NSI) source followed by tandem mass spectrometry (MS/MS) in Q Exactive PlusTM (Thermo

Fisher Scientific) coupled to the UPLC. The electrospray voltage applied was 2.0 kV. For MS scans, the m/z scan range was 350 to 1800. Intact peptides were detected in the orbitrap at a resolution of 70,000. Peptides were then selected for MS/MS in the orbitrap at a resolution of 17,500. Fixed first mass was set as 100 m/z. A data-dependent procedure that alternated between one MS scan followed by 20 MS/MS scans. In order to improve the effective utilization of mass spectrometry, the automatic gain control (AGC) is set to 5E4, the signal threshold is set to 10000 ions/s, the maximum injection time is set to 200 ms, and the dynamic exclusion time of the tandem mass scan is set to 30 seconds to avoid the repeat the scan of parent ion.

Database Search

The resulting MS/MS data were processed using Maxquant with an integrated Andromeda search engine (v.1.5.2.8). Tandem mass spectra were searched against the uniprot *Anas platyrhynchos* database concatenated with reverse decoy database. Trypsin/P was specified as cleavage enzyme allowing up to 2 missing cleavages. The mass tolerance for precursor ions was set as to 10 ppm in First search and 5 ppm in Main search, and the mass tolerance was set as 0.02 Da for fragment ions. TMT 10-plex was selected for protein quantification. False discovery rate (FDR) was adjusted to < 1% for protein identification.

TMT quantification

For TMT quantification, the ratios of the TMT reporter ion intensities in MS/MS

spectra (m/z 126–131) from raw data sets were used to calculate fold changes between samples. For each sample, the quantification was mean-normalized at peptide level to center the distribution of quantitative values. Protein quantitation were then calculated as the median ratio of corresponding unique or razor peptides for a given protein. Two-sample, two-sided T-tests were used to compare expression of proteins. A significance level of $P < 0.05$ was used for statistical testing and results were considered significant trend at $P < 0.1$.

Gene Ontology (GO) annotation

GO annotation proteome was derived from the UniProt-GOA database (www. http://www.ebi.ac.uk/GOA/). Firstly, Converting identified protein ID to UniProt ID and then mapping to GO IDs by protein ID. If some identified proteins were not annotated by UniProt-GOA database, the InterProScan soft would be used to annotated protein's GO functional based on protein sequence alignment method. Then proteins were classified by Gene Ontology annotation based on three categories: biological process, cellular component and molecular function.

16S rDNA sequencing

DNA was extracted from 180-220 mg of the cecal samples using a QIAampTM Fast DNA Stool Mini Kit (Qiagene, No. 51604) according to the manufacturer's instructions. Total DNA was quantified using a Thermo NanoDrop 2000 UV microscope spectrophotometer and 1% agarose gel electrophoresis. 16S rDNA high-throughput

sequencing was performed by Realbio Genomics Institute (Shanghai, China) using the Illumina Hiseq PE250 platform. The V3-V4 region of the 16S rDNA gene was amplified using the universal primers, 341F (CCTACGGGRSGCAGCAG) and 806R (GGACTACVVGGGTATCTAATC). The raw pair-end reads were merged and quality-filtered to remove tags with lengths < 220 nt, an average quality score of <20, and tags containing >3 ambiguous bases using PANDAseq (v2.9) [16]. Singletons and chimeras were removed, and the resulting quality-filtered sequences were clustered into 97% operational taxonomic units (OTUs) using USEARCH (v7.0.1090) in QIIME software. The Ribosomal Database Project (RDP) algorithm trained on the Greengenes database was used to classify each OTU (http://greengenes.lbl.gov). The open source software package QIIME (http://qiime.org) was used to measure alpha diversity (including the chao1, observed species and PD whole tree indices).

16S rDNA analysis

For 16S rDNA, the Wilcoxon rank sum test to evaluate changes in alpha diversity between H and L groups. Venn diagrams were constructed in R v3.1.0 using the Venn Diagram package. Principal component analysis (**PCA**) was used to assess the relationships between samples based on composition of the microbiota [17]. Linear discriminant analysis effect size (**LEfSe**), a metagenomic biomarker discovery approach, was used to identify differentially abundant taxa between H and L groups by using a Kruskal-Wallis rank sum test *P*-value threshold of 0.05 and a log-transformed linear discriminant analysis (**LDA**) score threshold of 2.

RESULTS

Duck performance and carcass traits

In our study, both the final body weight and the body weight gain over the study period decreased linearly with the increase of stocking density (Fig 1a, 1b). The feed/gain ratio increased linearly with increasing density (Fig 1c). Pectorals percentage was affected by stocking density as well, decreasing linearly with increasing stocking density (Fig 1d).

Fig 1. Duck performance and carcass traits. Data presented as means ± SE. n=6.

Biochemical indices of serum and pectorals

Both redox and lipid metabolism indices from serum and pectoral samples were affected by stocking density.

In redox indices, raising density was significantly associated serum MDA and LDH, as well as pectoral T-AOC (Table 1). Serum MDA increased linearly, while pectoral T-AOC decreased linearly with increasing stocking density (Table 1).

240 **Table 1 Redox related biochemical indices in serum and pectorals**

	Pectorals		Serum		
density/m^2	T-AOC	MDA	T-AOC	MDA	LDH
5	0.71±0.15^{AB}	2.12±0.60	15.79±2.30	7.39±0.54^{B}	9186.19±888.64^{A}
6	0.50±0.14^{AB}	1.42±0.59	13.03±5.35	7.47±0.51^{B}	9224.32±195.84^{A}
7	0.48±0.28^{AB}	1.74±0.77	10.77±5.51	7.10±0.58^{B}	10192.19±732.17^{A}
8	0.46±0.16^{AB}	1.37±0.44	14.55±1.23	8.68±0.05^{AB}	7864.87±814.26^{B}
9	0.22±0.08^{B}	1.87±0.46	11.51±3.95	9.57±1.56^{A}	9225.23±273.26^{A}
P-value					
ANOVA	0.015	0.176	0.278	0.008	0.001
Linear	0.023	0.490	0.253	0.038	0.238
Quadratic	0.069	0.148	0.269	0.068	0.470

241 Note: Total antioxidant capacity (T-AOC), malondialdehyde (MDA), lactate dehydrogenase (LDH).

242

243 Stocking density was also significantly altered lipid metabolism indices including
244 serum LPL, TG, TC, HDL-C and LDL-C, as well as pectoral LPL (Table 2).
245 Additionally, serum LDL-C increased linearly, and HDL-C had a linear increasing
246 trend with increasing density. Serum TG and pectoral LPL had quadratic trends
247 associated with stocking density (Table 2).

248

249 **Table 2 Lipid metabolism related biochemical indices**

	Pectorals	Serum				
Group	LPL	LPL	TG	TC	HDL-C	LDL-C
5	0.67±0.10^{BC}	2.76±0.62^{A}	1.01±0.22^{C}	4.14±0.32^{B}	4.01±0.30	3.24±0.60^{B}
6	0.99±0.23^{AB}	1.15±0.17^{B}	1.54±0.07^{B}	4.17±0.30^{B}	4.76±0.68	3.59±0.59^{B}
7	1.13±0.27^{A}	2.67±0.39^{A}	1.31±0.12^{BC}	4.13±0.15^{B}	4.41±0.83	4.83±0.73^{A}
8	0.84±0.30^{ABC}	2.52±0.79^{AB}	2.09±0.20^{A}	5.03±0.36^{A}	5.10±0.84	4.88±0.85^{A}
9	0.55±0.09^{C}	2.80±0.36^{A}	1.58±0.16^{B}	4.74±0.10^{A}	5.30±0.11	5.02±0.69^{A}
P-value						

ANOVA	0.003	<0.001	<0.001	<0.001	0.111	0.001
Linear	0.990	0.311	0.089	0.118	0.095	<0.001
Quadratic	0.098	0.506	0.050	0.302	0.250	<0.001

Note: lipoprotein lipase (LPL) triglyceride (TG), total cholesterol (TC), high-density lipoprotein cholesterol (HDL-C) and low-density lipoprotein cholesterol (LDL-C).

Proteins identification and comparison

In GO analysis, the most striking different pathways between H and L group were small molecule metabolic process, organic acid metabolic process, oxoacid metabolic process and carboxylic acid metabolic process. Pathways including oxidation-reduction process, cellular amino acid metabolic process and fatty acid metabolic process were significant altered as well (Fig 2). Many proteins involved in redox, lipid metabolism, protein turnover, DNA repair, and immunity were associated with stocking density (Table 3).

Fig 2. GO pathways enriched by H group. Log-transformed *P*-value is indicated the degree of difference between H group and L group.

268 **Table 3. Differentially expressed proteins identified under different stocking**

269 **density**

Accession ID[a]	Annotation	Gene	H:L[b]	*P*-value
	Redox related proteins			
U3I9D6	DDRGK domain containing 1	DDRGK	1.218	0.010
MT	Metallothionein	N/A	1.332	0.014
U3ID81	Regucalcin	RGN	0.706	0.025
R0M3U9	Catalase	Anapl_09675	0.882	0.051
	Lipid metabolism related proteins			
U3IAY7	Acyl-CoA dehydrogenase, long chain	ACADL	1.154	0.040
U3I7T9	Acyl-CoA synthetase family member 2	ACSF2	1.103	0.032
U3J928	Acyl-coenzyme A oxidase	ACOX1	1.098	0.007
U3I7I1	2-hydroxyacyl-CoA lyase 1	HACL1	1.143	0.095
	Protein turnover related proteins			
U3I9U9	Pyridoxal kinase	PDXK	1.324	0.011
U3IHG9	Ribosomal protein S20	RPS20	1.103	0.045
U3I350	Aspartyl-tRNA synthetase	DARS	1.119	0.096
U3J7Z7	Asparaginyl-tRNA synthetase	NARS	0.904	0.068
	DNA repair related proteins			
U3IUN7	RNA binding motif protein, X-linked	RBMX	1.136	0.068
U3IUB7	Lamin B2	LMNB2	1.119	0.076
	Immunity related proteins			
R0K747	Macrophage mannose receptor 1	Anapl_08603	1.170	0.004
Q6JWQ2	MHC class I antigen alpha chain	Anpl-U	0.785	0.021

270

Antioxidant related proteins such as regucalcin and catalase were downregulated in H group. Oxidative response related proteins like DDRGK domain containing 1 and metallothionein were enhanced in H group.

Fatty acid synthesis protein acyl-CoA synthetase family member 2 (ACSF2) was enriched in high stockind density. Fatty acid oxidation connected proteins including acyl-CoA dehydrogenase long chain (ACADL), acyl-coenzyme A oxidase (ACOX1) and 2-hydroxyacyl-CoA lyase 1 (HACL1) were enriched in the H group.

Protein turnover related proteins including Ribosomal protein S20, Pyridoxal kinase and aspartyl-tRNA synthetase (DARS2) were elevated while Asparaginyl-tRNA synthetase was reduced in H group.

In DNA repair involved proteins, Both RNA-binding motif protein X-linked (RBMX) and Lamin B2 showed enhancing trends in H group. The immunity associated macrophage mannose receptor (MR) 1 was elevated, while Major histocompatibility complex (MHC) class I antigen α chain was decreased in the H group.

16S rDNA analysis of cecal microbiota

Microbiota PCA analysis showed a clear separation of samples from the H group and samples from the L group (Fig 3a). The H group and L group had 290 bacterial taxa in common, while the H group and L group had 35 and 13 unique taxa, respectively (Fig 3b).

Fig. 3 PCA and Veen chart of microbiota. a, PCA diagram; b, Veen chart.

LEfSe analysis, revealed higher relative abundance of *Firmicutes* and *Phascolarctobacterium* in the H group, while *Bacteroidia*, *Bacteroidales*, *Thermoplasmata*, *Methanomassiliicoccales*, *Methanomassiliicoccus* and *Methanomassiliicoccaceae* were more abundant in the L group (Fig 4a, 4b). Additionally, the H group had elevated *Lachnospiraceae* and *Ruminococcaceae* lower abundance of *Butyricimonas*, *Desulfovibrionaceae*, *Alistipes* and *Clostridiales* (Fig 5). Overall, the ratio of *Firmicutes* to *Bacteroidetes* in the H group was higher than in the L group ($P = 0.058$).

Fig 4. Bacterial taxa in H or L groups by LEfSe analysis. Phylogenetic relationships among significant bacterial biomarkers are indicated in the cladogram (top). Log-transformed linear discriminant analysis (LDA) scores of the significant biomarkers are indicated the bar chart (bottom).

Fig 5. Relative abundance of anti-inflammatory bacterial taxa in H or L groups.

DISCUSSION

Previous studies have indicated that that high raising density has negative influences on physiology and overall meat production [2-4]. This study showed a linear decrease

311 of BW with increasing stocking density. Similarly, breast muscle was depressed by
312 increasing stocking density. Which was consistent with the formerly research that
313 increasing stocking density decreased breast fillet weight and its relative yield [18].

314 Increased density is associated with impaired antioxidant capacity, including
315 decreasing total glutathione concentration and the glutathione (GSH): oxidized
316 glutathione (GSSG) ratio [2]. Liver antioxidants including superoxide dismutase (SOD),
317 catalase (CAT), GSH have previously been found to be reduced under high raising
318 density [19]. In this study, enhancing stocking density increased serum MDA and
319 decreased pectoral T-AOC. In proteomic analysis of this study, regucalcin and catalase
320 expression was reduced in high density group. Catalases are involved in protecting cells
321 from the damaging effects of ROS [20], while regucalcin is a calcium-binding protein
322 with multiple roles that include calcium homeostasis, anti-oxidative, anti-apoptosis, and
323 anti-proliferation [21]. Decreases in these proteins indicates that high stocking density
324 may reduce duck anti-oxidant capacity.

325 High stocking density increases blood oxidative stress, including acute phase
326 proteins, heat shock protein 70, and circulating corticosterone [22]. In current study,
327 high stocking density had higher expressions of DDRGK domain containing 1,
328 metallothionein, DARS2 and RBMX. DDRGK domain containing 1 and
329 metallothionein were enriched in high density group. DDRGK1 is an endoplasmic
330 reticulum membrane protein and plays an important role in maintaining the homeostasis
331 of endoplasmic reticulum [23]. Metallothionein is an essential protein for the protection
332 of cells against reactive oxygen species (ROS) [24]. Therefore, metallothionein can

333 neutralize ROS and protect host from oxidative stress. A previous study found that loss
334 of mitochondrial DARS2 leads to the activation of various stress responses in a tissue-
335 specific manner independently of respiratory chain deficiency [25]. The RBMX is a
336 nuclear protein that is involved in alternative splicing of RNA [26]. It is able to confer
337 resistance to DNA damage [27]. Enhancement of these proteins suggests oxidative
338 stress of Peking ducks under high stocking density.

339 Lipid storage is essential for protection against ROS toxicity [28]. The lipogenesis
340 occurs in liver most exclusively, especially to waterfowls [29]. High stocking density
341 was previously associated higher hepatic TG storage [30]. This study showed serum
342 LDL-C increased with density incrementing. Moreover, high density group elevated
343 ACSF2 expression. Acetyl-CoA synthetase catalyzes the formation of acetyl-CoA from
344 acetate, CoA and ATP and participates in various metabolic pathways, including fatty
345 acid and cholesterol synthesis and the tricarboxylic acid cycle [31]. ACSF2 belongs to
346 the acyl-CoA synthetase family, activating fatty acids by forming a thioester bond with
347 CoA [32]. Therefore, the increasing lipid biosynthesis may be the self-protection
348 mechanism of Peking ducks under oxidative stress.

349 ROS are considered to be involved in the progression of non-alcoholic fatty liver
350 disease (NAFLD) [33]. Interestingly, fatty liver production in waterfowls are fairly
351 similar to human NAFLD [34]. Therefore, waterfowls can be a good model for liver
352 steatosis research. In current study, ACADL, ACOX1 and HACL1 were enriched in
353 high stocking density group. ACADL is a key enzyme participating in fatty acid
354 oxidation [35]. Similary, ACOX1 are involved in β-oxidation in the liver [36]. HACL1

355 has two important roles in α-oxidation, the degradation of phytanic acid and shortening
356 of 2-hydroxy long-chain fatty acids so that they can be degraded further by β-oxidation
357 [37]. It has been reported that inhibition of β-oxidation decreases NADPH levels and
358 increases ROS levels [38]. Therefore, elevation of these proteins may protect ducks
359 from oxidative stress. It is increasingly recognized that the composition of the gut
360 microbiota plays a critical role in influencing predisposition to chronic liver disorders
361 such as NAFLD [12]. Samples from high stocking density had high levels of
362 *Lachnospiraceae.* Interestingly, high *Lachnospiraceae* abundance was observed in
363 patients with nonalcoholic steatohepatitis [39]. *Ruminococcaceae* and *Alistipes* were
364 depleted in the high density group. Cirrhotic patients were previously shown to have
365 lower *Ruminococcaceae* (7α-dehydroxylating bacteria) abundance compared to healthy
366 patients [40]. In addition, *Alistipes* was significantly more abundant in the gut
367 microbiota of healthy subjects compared to NAFLD patients [41].

368 Immunity can be regulated by oxidative stress. A decreased broiler bursa weight was
369 previously reported to be associated with higher stocking densities [2]. DDRGK
370 domain-containing protein 1 and Macrophage mannose receptor (MR) expression was
371 higher in high density compared to the low density group. DDRGK1 is also an
372 important regulatory protein of NF-κB [42]. Recent study found MR can protect against
373 ROS burst [43]. Increase of these proteins reflects the immune response status Peking
374 ducks under high stocking density. MHC class I antigen α chain was decreased under
375 high stocking density. MHC class I plays a crucial role in immunity by capturing
376 peptides for presentation to T cells and natural killer (NK) cells [44]. Dysregulation of

MHC class I was correlated with unfolded protein response (UPR) and endoplasmic reticulum (ER) stress [45]. Upregulation of these proteins in the high density group suggests the immune adaption to high stocking. Moreover, high stocking density has been previously associated with adverse effects on the chicken intestinal commensal bacteria [4]. In the current study, *Phascolarctobacterium* was enriched, while *Bacteroidales, Butyricimonas* and *Alistipe* are depleted in high density group. A previous study found that *Phascolarctobacterium* was significantly correlated with systemic inflammatory cytokines [46]. Besides, depletion of *Bacteroidales* has previously been associated with disease status [47]. Additionally, reduction in *Butyricimonas* is associated with increased proinflammatory gene expression [48]. Studies confirm that patients with IBD and *Clostridium difcile* infection have a lower abundance of *Alistipe* than their healthy counterparts [49]. The current study showed higher *Firmicutes* to *Bacteroidetes* ratio in high density group. The microbiota of irritable bowel syndrome (IBS) patients, compared with controls, had a 2-fold increased ratio of the *Firmicutes* to *Bacteroidetes* [50]. Bile acids (BAs) are important metabolites of the microbiome and can modulate the composition of the gut microbiota directly or indirectly through activation of the innate immune system [51]. Bile acid plays a crucial role in control of inflammation and NAFLD [52]. Samples from the high stocking density group had higher levels of *Ruminococcaceae* and lower abundance of *Desulfovibrionaceae*, and *Clostridiales* compared to low density group. Cholesterol 7α-hydroxylase (CYP7A1) is the enzyme responsible for catalyzing the first and rate-limiting step in the classical bile acid synthetic pathway [53]. Futhermore, an inverse

399 relationship between Cyp7a1 expression and *Ruminococcaceae* abundance has been
400 previously demonstrated [19]. A study found enriched *Desulfovibrionaceae* was
401 accompanied by increased hepatic taurine-conjugated cholic acid and β-muricholic acid,
402 which were the main constituent of bile acid pool [54]. *Clostridiale* was positively
403 correlated with muricholic acid as well [19]. A loss of bacteria belonging to the
404 *Clostridiales* order was correlated with a disturbance in the bile-microbial axis [55].
405 Therefore, alternations of bacteria showed a decrease trend in bile acid synthesis.

406 In conclusion, high stocking density caused oxidative stress, which involved in
407 alternation of gut-liver axis (Fig 6).

408

409 **Fig 6. Graphic summary of liver proteome and gut microbiota alternations under**
410 **high stocking density.**

411

412 # Acknowledgements

413 This research was supported by the System for Poultry Production Technology,
414 Beijing Agriculture Innovation Consortium (Project Number: BAIC04-2017).

415

416

417

418

References:

1. Buijs S, Keeling LJ, Vangestel C, Baert J, Vangeyte J, et al. (2010) Resting or hiding? Why broiler chickens stay near walls and how density affects this. Applied Animal Behaviour Science 124: 97-103.

2. Simitzis PE, Kalogeraki E, Goliomytis M, Charismiadou MA, Triantaphyllopoulos K, et al. (2012) Impact of stocking density on broiler growth performance, meat characteristics, behavioural components and indicators of physiological and oxidative stress. Br Poult Sci 53: 721-730.

3. Xie M, Jiang Y, Tang J, Wen ZG, Huang W, et al. (2014) Effects of stocking density on growth performance, carcass traits, and foot pad lesions of White Pekin ducks. Poult Sci 93: 1644-1648.

4. Cengiz O, Koksal BH, Tatli O, Sevim O, Ahsan U, et al. (2015) Effect of dietary probiotic and high stocking density on the performance, carcass yield, gut microflora, and stress indicators of broilers. Poult Sci 94: 2395-2403.

5. Yin LY, Wang ZY, Yang HM, Xu L, Zhang J, et al. (2017) Effects of stocking density on growth performance, feather growth, intestinal development, and serum parameters of geese. Poult Sci 96: 3163-3168.

6. Zhang YR, Zhang LS, Wang Z, Liu Y, Li FH, et al. (2018) Effects of stocking density on growth performance, meat quality and tibia development of Pekin ducks. Anim. Sci. J. 00:1–6.

7. Tong HB, Lu J, Zou JM, Wang Q, Shi SR (2012) Effects of stocking density on growth performance, carcass yield, and immune status of a local chicken breed. Poult

441 Sci 91: 667-673.

442 8. Li JH, Miao ZQ, Tian WX, Yang Y, Wang JD, et al. (2017) Effects of different
443 rearing systems on growth, small intestinal morphology and selected indices of
444 fermentation status in broilers. Animal Science Journal 88: 900-908.

445 9. Naderi M, Keyvanshokooh S, Salati AP, Ghaedi A (2017) Effects of chronic high
446 stocking density on liver proteome of rainbow trout (Oncorhynchus mykiss). Fish
447 Physiol Biochem 43: 1373-1385.

448 10. Kpundeh MD, Xu P, Yang H, Qiang J, He J (2013) Stocking densities and chronic
449 zero culture water exchange stress' effects on biological performances, hematological
450 and serum biochemical indices of GIFT tilapia juveniles (Oreochromis niloticus). J.
451 Aquac. Res. Development 4: 189.

452 11. Yeoman CJ, White BA (2014) Gastrointestinal tract microbiota and probiotics in
453 production animals. Annu Rev Anim Biosci 2: 469-486.

454 12. Leung C, Rivera L, Furness JB, Angus PW (2016) The role of the gut microbiota
455 in NAFLD. Nat Rev Gastroenterol Hepatol 13: 412-425.

456 13. Shen LF, Chen YJ, Liu KM, Haddad A, Song IW, et al. (2017) Role of S-
457 Palmitoylation by ZDHHC13 in Mitochondrial function and Metabolism in Liver. Sci
458 Rep 7: 2182.

459 14. Tang J, Hegeman MA, Hu J, Xie M, Shi W, et al. (2017) Severe riboflavin
460 deficiency induces alterations in the hepatic proteome of starter Pekin ducks. Br J
461 Nutr 118: 641-650.

462 15. Whitson JA, Wilmarth PA, Klimek J, Monnier VM, David L, et al. (2017)

463 Proteomic analysis of the glutathione-deficient LEGSKO mouse lens reveals
464 activation of EMT signaling, loss of lens specific markers, and changes in stress
465 response proteins. Free Radic Biol Med 113: 84-96.
466 16. Masella AP, Bartram AK, Truszkowski JM, Brown DG, Neufeld JD (2012)
467 PANDAseq: paired-end assembler for illumina sequences. BMC Bioinformatics 13:
468 31.
469 17. Sanders JG, Beichman AC, Roman J, Scott JJ, Emerson D, et al. (2015) Baleen
470 whales host a unique gut microbiome with similarities to both carnivores and
471 herbivores. Nat Commun 6: 8285.
472 18. Dozier WR, Thaxton JP, Purswell JL, Olanrewaju HA, Branton SL, et al. (2006)
473 Stocking density effects on male broilers grown to 1.8 kilograms of body weight.
474 Poult Sci 85: 344-351.
475 19. Liu H, Rocha CS, Dandekar S, Wan YY (2016) Functional analysis of the
476 relationship between intestinal microbiota and the expression of hepatic genes and
477 pathways during the course of liver regeneration. J Hepatol 64: 641-650.
478 20. Bhattacharyya A, Chattopadhyay R, Mitra S, Crowe SE (2014) Oxidative stress: an
479 essential factor in the pathogenesis of gastrointestinal mucosal diseases. Physiol Rev
480 94: 329-354.
481 21. Pillai H, Parmar MS, Shende AM, Thomas J, Kartha HS, et al. (2017) Effect of
482 supplementation of recombinant Regucalcin in extender on cryopreservation of
483 spermatozoa of water buffalo (Bubalus bubalis). Mol Reprod Dev 84: 1133-1139.
484 22. Najafi P, Zulkifli I, Jajuli NA, Farjam AS, Ramiah SK, et al. (2015) Environmental

485 temperature and stocking density effects on acute phase proteins, heat shock protein
486 70, circulating corticosterone and performance in broiler chickens. Int J Biometeorol
487 59: 1577-1583.
488 23. Liu J, Wang Y, Song L, Zeng L, Yi W, et al. (2017) A critical role of DDRGK1 in
489 endoplasmic reticulum homoeostasis via regulation of IRE1 alpha stability. Nat
490 Commun 8:14186.
491 24. Carrera G, Paternain JL, Carrere N, Folch J, Courtade-Saidi M, et al. (2003) Hepatic
492 metallothionein in patients with chronic hepatitis C: Relationship with severity of
493 liver disease and response to treatment. Am J Gastroenterol 98: 1142-1149.
494 25. Dogan SA, Pujol C, Maiti P, Kukat A, Wang S, et al. (2014) Tissue-Specific Loss
495 of DARS2 Activates Stress Responses Independently of Respiratory Chain
496 Deficiency in the Heart. Cell Metab. 19: 458-469.
497 26. Dai M, Liu Y, Nie X, Zhang J, Wang Y, et al. (2015) Expression of RBMX in the
498 Light-Induced Damage of Rat Retina In Vivo. Cell Mol Neurobiol 35: 463-471.
499 27. Adamson B, Smogorzewska A, Sigoillot FD, King RW, Elledge SJ (2012) A
500 genome-wide homologous recombination screen identifies the RNA-binding protein
501 RBMX as a component of the DNA-damage response. Nat Cell Biol 14: 318-328.
502 28. Bensaad K, Favaro E, Lewis CA, Peck B, Lord S, et al. (2014) Fatty acid uptake
503 and lipid storage induced by HIF-1alpha contribute to cell growth and survival after
504 hypoxia-reoxygenation. Cell Rep 9: 349-365.
505 29. Mourot J, Guy G, Lagarrigue S, Peiniau P, Hermier D (2000) Role of hepatic
506 lipogenesis in the susceptibility to fatty liver in the goose (Anser anser). Comp

507 Biochem Physiol B Biochem Mol Biol 126: 81-87.

508 30. Menezes C, Ruiz-Jarabo I, Antonio Martos-Sitcha J, Toni C, Salbego J, et al. (2015)
509 The influence of stocking density and food deprivation in silver catfish (Rhamdia
510 quelen): A metabolic and endocrine approach. Aquaculture 435: 257-264.

511 31. Fujino T, Kondo J, Ishikawa M, Morikawa K, Yamamoto TT (2001) Acetyl-CoA
512 synthetase 2, a mitochondrial matrix enzyme involved in the oxidation of acetate. J
513 Biol Chem 276: 11420-11426.

514 32. Yu S, Wei W, Xia M, Jiang Z, He D, et al. (2016) Molecular characterization,
515 alternative splicing and expression analysis of ACSF2 and its correlation with egg-
516 laying performance in geese. Anim Genet 47: 451-462.

517 33. Koliaki C, Szendroedi J, Kaul K, Jelenik T, Nowotny P, et al. (2015) Adaptation of
518 hepatic mitochondrial function in humans with non-alcoholic fatty liver is lost in
519 steatohepatitis. Cell Metab 21: 739-746.

520 34. Ray K (2013) NAFLD-the next global epidemic. Nat Rev Gastroenterol Hepatol
521 10: 621.

522 35. Chen T, Liu J, Li N, Wang S, Liu H, et al. (2015) Mouse SIRT3 attenuates
523 hypertrophy-related lipid accumulation in the heart through the deacetylation of
524 LCAD. PLoS One 10: e118909.

525 36. Osumi T, Hashimoto T, Ui N (1980) Purification and properties of acyl-CoA
526 oxidase from rat liver. J Biochem 87: 1735-1746.

527 37. Lonsdale D (2015) Thiamine and magnesium deficiencies: keys to disease. Med
528 Hypotheses 84: 129-134.

529 38. Pike LS, Smift AL, Croteau NJ, Ferrick DA, Wu M (2011) Inhibition of fatty acid
530 oxidation by etomoxir impairs NADPH production and increases reactive oxygen
531 species resulting in ATP depletion and cell death in human glioblastoma cells.
532 Biochim Biophys Acta 1807: 726-734.
533 39. Del CF, Nobili V, Vernocchi P, Russo A, Stefanis C, et al. (2017) Gut microbiota
534 profiling of pediatric nonalcoholic fatty liver disease and obese patients unveiled by
535 an integrated meta-omics-based approach. Hepatology 65: 451-464.
536 40. Kakiyama G, Pandak WM, Gillevet PM, Hylemon PB, Heuman DM, et al. (2013)
537 Modulation of the fecal bile acid profile by gut microbiota in cirrhosis. J Hepatol 58:
538 949-955.
539 41. Jiang W, Wu N, Wang X, Chi Y, Zhang Y, et al. (2015) Dysbiosis gut microbiota
540 associated with inflammation and impaired mucosal immune function in intestine of
541 humans with non-alcoholic fatty liver disease. Sci Rep 5: 8096.
542 42. Xi P, Ding D, Zhou J, Wang M, Cong YS (2013) DDRGK1 regulates NF-kappaB
543 activity by modulating IkappaBalpha stability. PLoS One 8: e64231.
544 43. Hagert C, Sareila O, Kelkka T, Jalkanen S, Holmdahl R (2018) The Macrophage
545 Mannose Receptor Regulate Mannan-Induced Psoriasis, Psoriatic Arthritis, and
546 Rheumatoid Arthritis-Like Disease Models. Front Immunol 9: 114.
547 44. Pymm P, Illing PT, Ramarathinam SH, O'Connor GM, Hughes VA, et al. (2017)
548 MHC-I peptides get out of the groove and enable a novel mechanism of HIV-1 escape.
549 Nat Struct Mol Biol 24: 387-394.
550 45. Osorio F, Tavernier SJ, Hoffmann E, Saeys Y, Martens L, et al. (2014) The

551 unfolded-protein-response sensor IRE-1alpha regulates the function of CD8alpha+
552 dendritic cells. Nat Immunol 15: 248-257.
553 46. Polansky O, Sekelova Z, Faldynova M, Sebkova A, Sisak F, et al. (2016) Important
554 Metabolic Pathways and Biological Processes Expressed by Chicken Cecal
555 Microbiota. Appl Microbiol Biotechnol 82: 1569-1576.
556 47. Gevers D, Kugathasan S, Denson LA, Vazquez-Baeza Y, Van Treuren W, et al.
557 (2014) The Treatment-Naive Microbiome in New-Onset Crohn's Disease. Cell Host
558 Microbe. 15: 382-392.
559 48. Jangi S, Gandhi R, Cox LM, Li N, von Glehn F, et al. (2016) Alterations of the
560 human gut microbiome in multiple sclerosis. Nat Commun 7: 12015.
561 49. Mancabelli L, Milani C, Lugli GA, Turroni F, Cocconi D, et al. (2017) Identification
562 of universal gut microbial biomarkers of common human intestinal diseases by meta-
563 analysis. FEMS Microbiol. Ecol. 93: fix153.
564 50. Rajilic-Stojanovic M, Biagi E, Heilig HG, Kajander K, Kekkonen RA, et al. (2011)
565 Global and deep molecular analysis of microbiota signatures in fecal samples from
566 patients with irritable bowel syndrome. Gastroenterology 141: 1792-1801.
567 51. Ridlon JM, Kang DJ, Hylemon PB, Bajaj JS (2014) Bile acids and the gut
568 microbiome. Curr Opin Gastroenterol 30: 332-338.
569 52. Chavez-Talavera O, Tailleux A, Lefebvre P, Staels B (2017) Bile Acid Control of
570 Metabolism and Inflammation in Obesity, Type 2 Diabetes, Dyslipidemia, and
571 Nonalcoholic Fatty Liver Disease. Gastroenterology 152: 1679-1694.
572 53. Luo J, Ko B, Elliott M, Zhou M, Lindhout DA, et al. (2014) A nontumorigenic

573 variant of FGF19 treats cholestatic liver diseases. Sci Transl Med 6: 100r-247r.

574 54. Sheng L, Jena PK, Liu HX, Kalanetra KM, Gonzalez FJ, et al. (2017) Gender
575 Differences in Bile Acids and Microbiota in Relationship with Gender Dissimilarity
576 in Steatosis Induced by Diet and FXR Inactivation. Sci Rep 7: 1748.

577 55. Pereira-Fantini PM, Bines JE, Lapthorne S, Fouhy F, Scurr M, et al. (2016) Short
578 bowel syndrome (SBS)-associated alterations within the gut-liver axis evolve early
579 and persist long-term in the piglet model of short bowel syndrome. J Gastroenterol
580 Hepatol 31: 1946-1955.

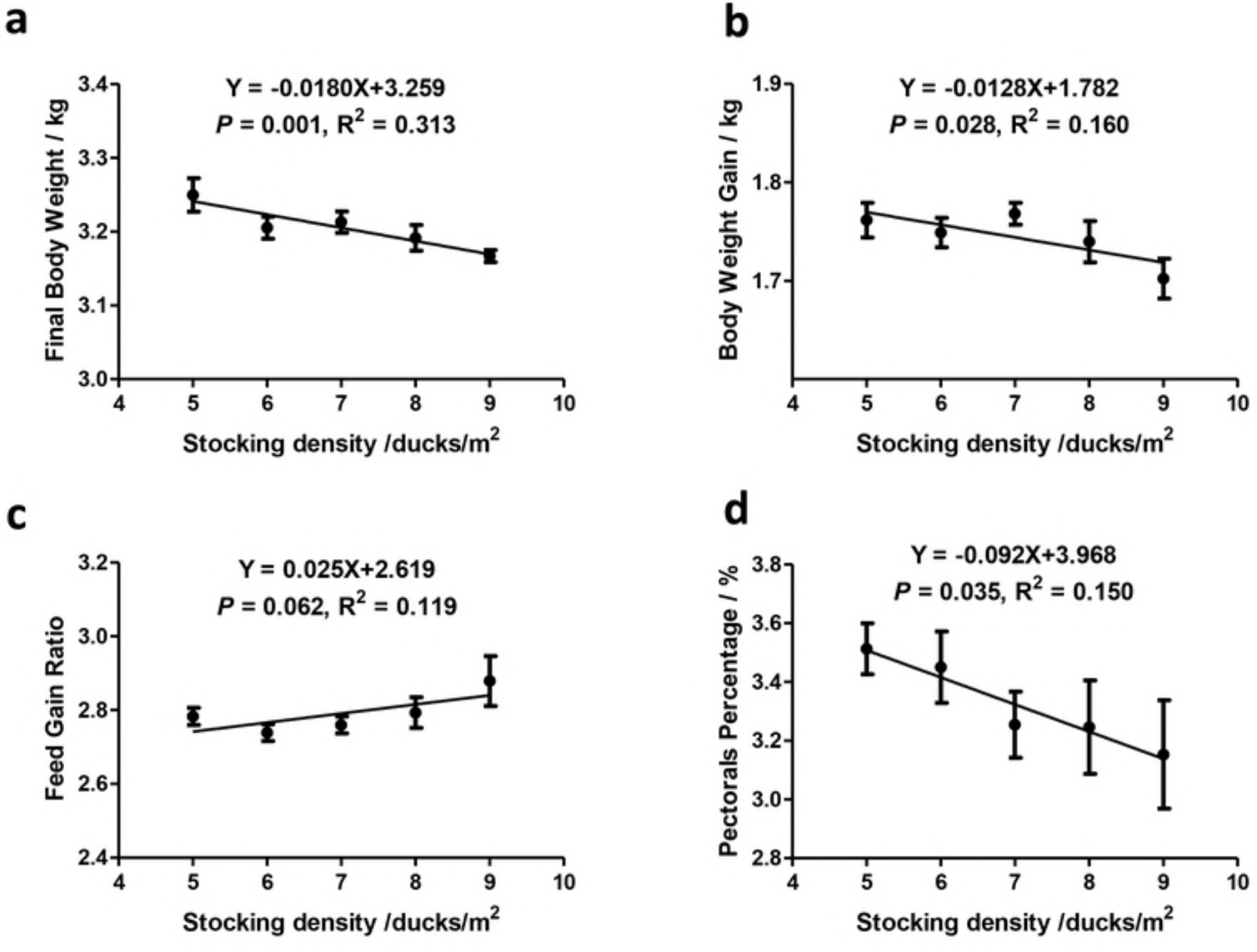
a
Y = -0.0180X+3.259
P = 0.001, R2 = 0.313
Final Body Weight / kg
3.4
3.3
3.2
3.1
3.0
4
5
6
7
8
9
10
Stocking density /ducks/m2
b
Y = -0.0128X+1.782
P = 0.028, R2 = 0.160
Body Weight Gain / kg
1.9
1.8
1.7
Stocking density /ducks/m2
c
Y = 0.025X+2.619
P = 0.062, R2 = 0.119
Feed Gain Ratio
3.2
3.0
2.8
2.6
2.4
Stocking density /ducks/m2
d
Y = -0.092X+3.968
P = 0.035, R2 = 0.150
Pectorals Percentage / %
3.8
3.6
3.4
3.2
3.0
2.8
Stocking density /ducks/m2

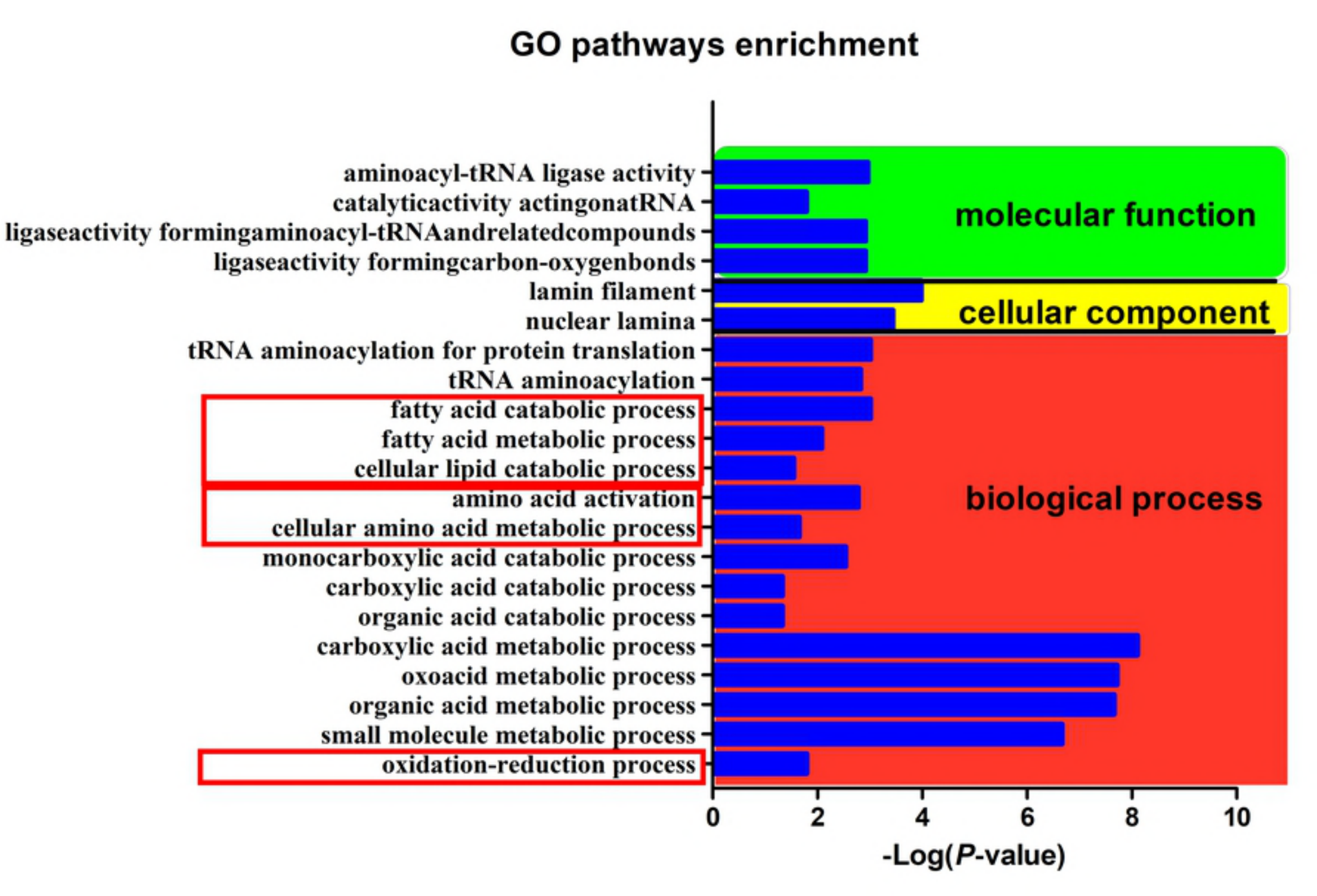
GO pathways enrichment
aminoacyl-tRNA ligase activity
catalyticactivity actingonatRNA
ligaseactivity formingaminoacyl-tRNAandrelatedcompounds
ligaseactivity formingcarbon-oxygenbonds
lamin filament
nuclear lamina
tRNA aminoacylation for protein translation
tRNA aminoacylation
fatty acid catabolic process
fatty acid metabolic process
cellular lipid catabolic process
amino acid activation
cellular amino acid metabolic process
monocarboxylic acid catabolic process
carboxylic acid catabolic process
organic acid catabolic process
carboxylic acid metabolic process
oxoacid metabolic process
organic acid metabolic process
small molecule metabolic process
oxidation-reduction process
molecular function
cellular component
biological process
0
2
4
6
8
10
-Log(P-value)

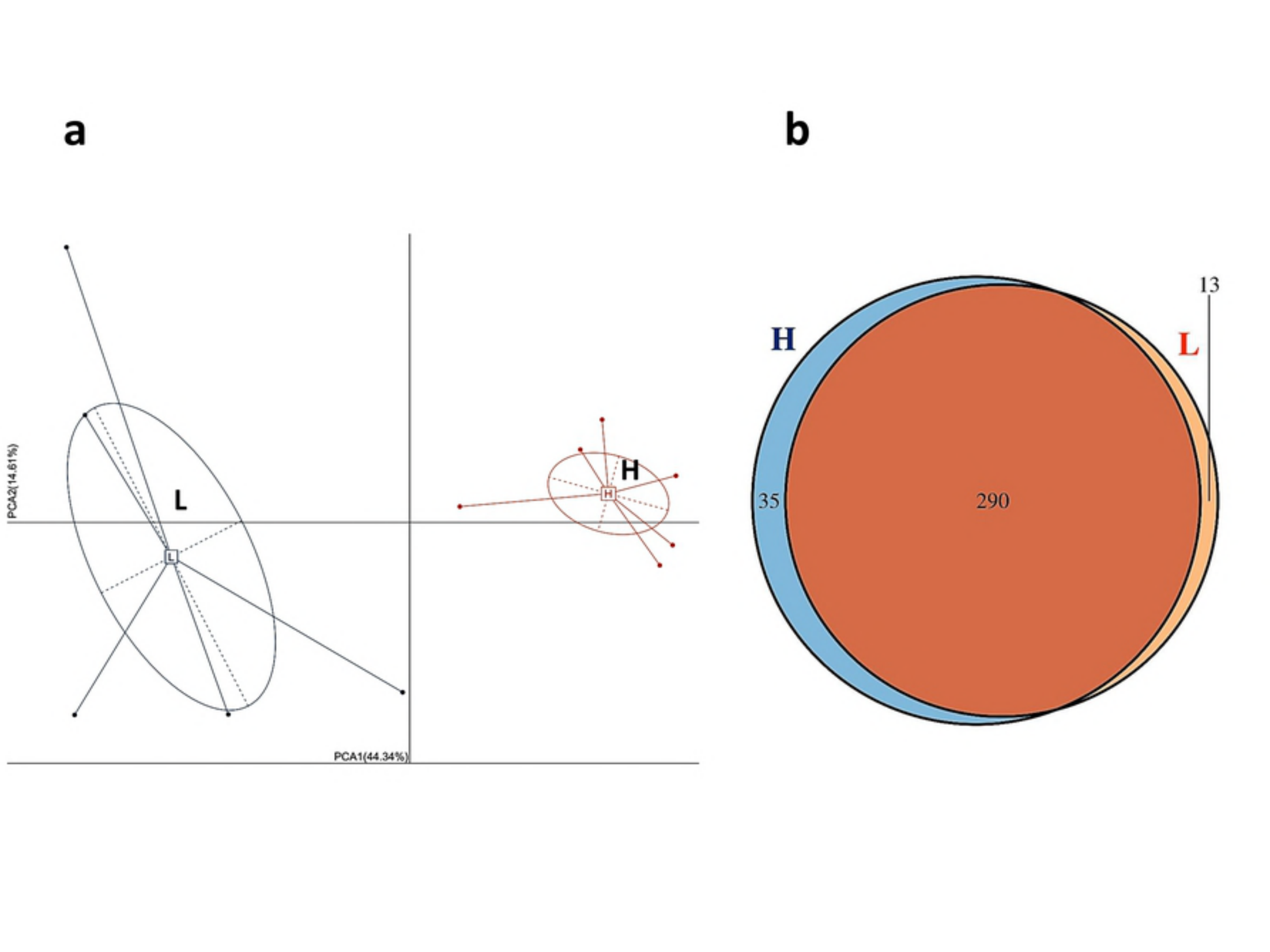
a
b
PCA2(14.61%)
PCA1(44.34%)
L
H
H
L
13
35
290

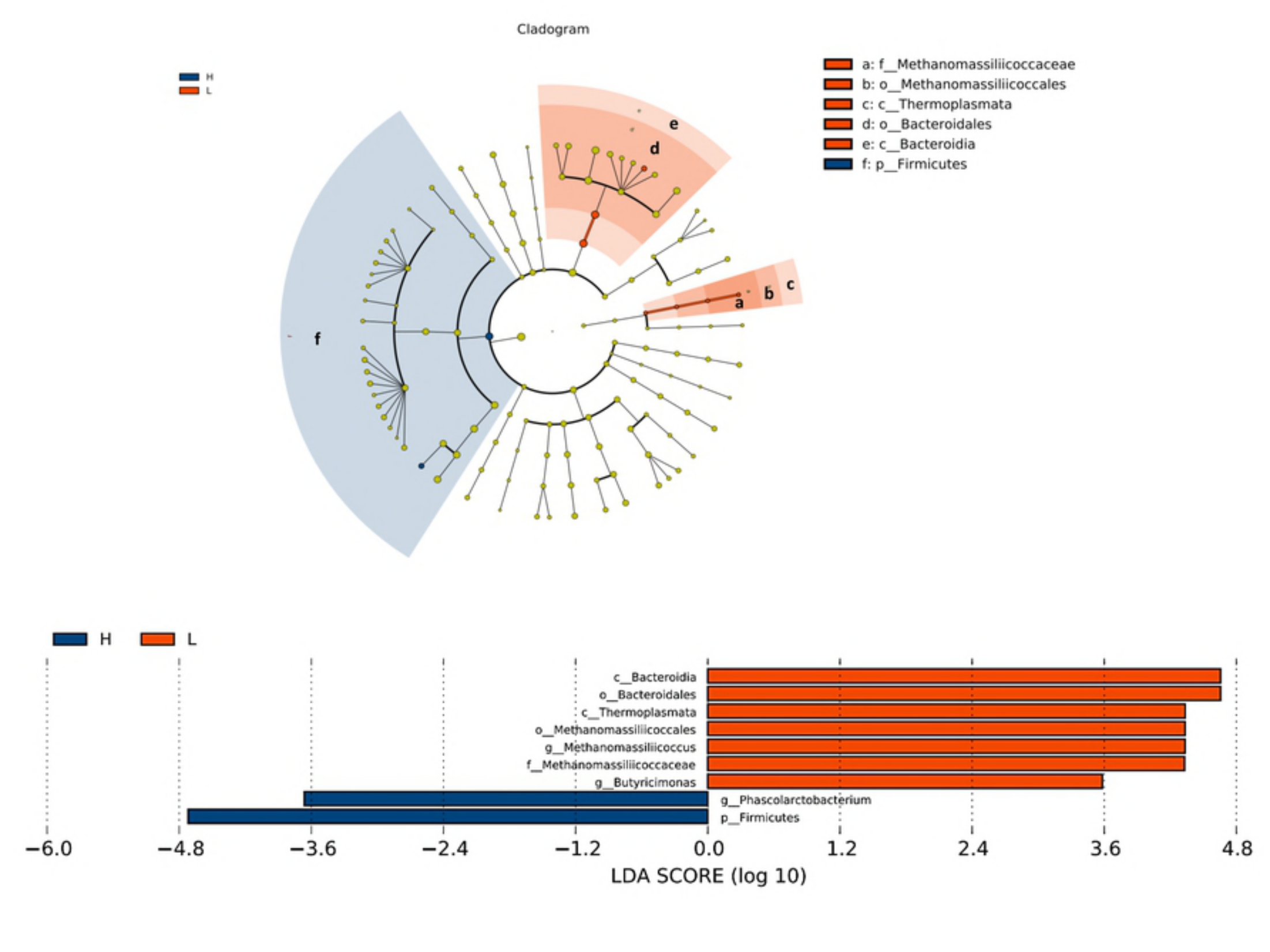
Cladogram
H
L
a: f__Methanomassiliicoccaceae
b: o__Methanomassiliicoccales
c: c__Thermoplasmata
d: o__Bacteroidales
e: c__Bacteroidia
f: p__Firmicutes
a
b
c
d
e
f
H
L
c__Bacteroidia
o__Bacteroidales
c__Thermoplasmata
o__Methanomassiliicoccales
g__Methanomassiliicoccus
f__Methanomassiliicoccaceae
g__Butyricimonas
g__Phascolarctobacterium
p__Firmicutes
−6.0
−4.8
−3.6
−2.4
−1.2
0.0
1.2
2.4
3.6
4.8
LDA SCORE (log 10)

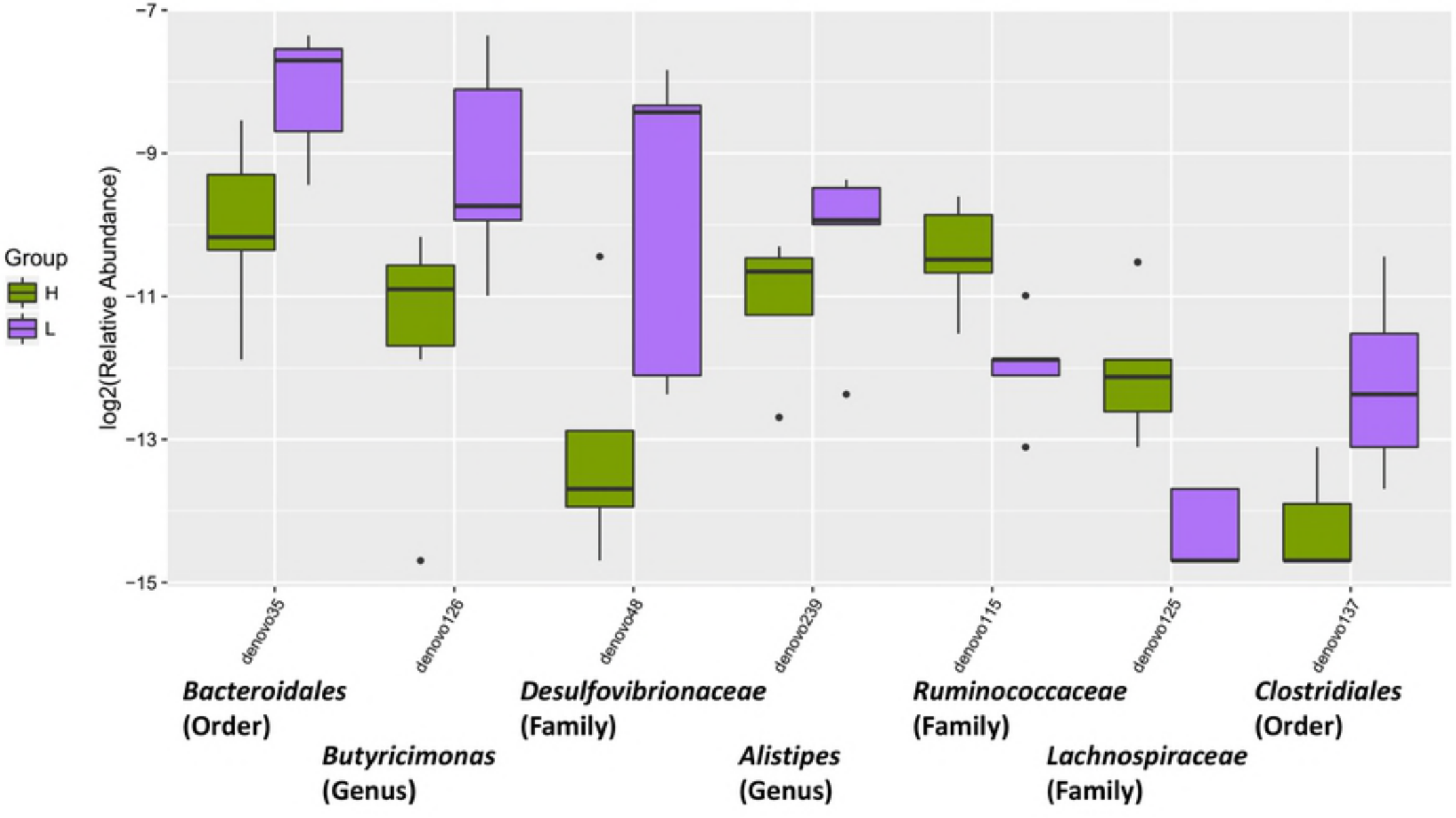
Group
H
L
log2(Relative Abundance)
−7
−9
−11
−13
−15
denovo35
denovo126
denovo48
denovo239
denovo115
denovo125
denovo137
Bacteroidales
(Order)
Butyricimonas
(Genus)
Desulfovibrionaceae
(Family)
Alistipes
(Genus)
Ruminococcaceae
(Family)
Lachnospiraceae
(Family)
Clostridiales
(Order)